TiH_2-40Nb Alloy as Alternative to Ti-40Nb Alloy for Bone Implant: A Comparative Study

Ahmad Farrahnoor
Mechanical Engineering Studies, Universiti Teknologi MARA Cawangan Pulau Pinang, Permatang Pauh Campus

Anis Fatehah Sa'aidi
Mechanical Engineering Studies, Universiti Teknologi MARA Cawangan Pulau Pinang, Permatang Pauh Campus

Muhammad Shamel Shaipudin
Mechanical Engineering Studies, Universiti Teknologi MARA Cawangan Pulau Pinang, Permatang Pauh Campus

Zuhailawati Hussain
Biomaterials Niche Area, School of Materials and Mineral Resources Engineering, Universiti Sains Malaysia, Engineering Campus

出版情報：Evergreen. 13 (3), pp.1025-1032, 2026-09. 九州大学グリーンテクノロジー研究教育センター
バージョン：

TiH_2-40Nb Alloy as Alternative to Ti-40Nb Alloy for Bone Implant: A Comparative Study

Ahmad Farrahnoor[1,*], Anis Fatehah Sa'aidi[1],
Muhammad Shamel Shaipudin[1], Zuhailawati Hussain[2]

[1]Mechanical Engineering Studies, Universiti Teknologi MARA Cawangan Pulau Pinang, Permatang Pauh Campus, 13500 Seberang Prai, Pulau Pinang, Malaysia
[2]Biomaterials Niche Area, School of Materials and Mineral Resources Engineering, Universiti Sains Malaysia, Engineering Campus, 14300 Nibong Tebal, Pulau Pinang, Malaysia

*Author to whom correspondence should be addressed:
E-mail: farra728@uitm.edu.my

(Received April 21, 2025; Revised June 16, 2026; Accepted July 31, 2026)

Abstract: The bioactivity of TiH_2 as a starting material in the preparation of β-phase stabilized Ti alloys, remains largely unexplored. This paper examines the hydrogen impact on apatite formation on the TiH_2-40Nb alloy's surface. The TiH_2-40Nb alloy was synthesized using mechanical alloying and powder metallurgy techniques, including cold powder compaction and sintering process. The alloy's bioactivity was assessed by immersing samples in Hank's Balanced Salt Solution (HBSS) for 30 days, followed by characterization using weight gain analysis, pH measurement, and scanning electron microscopy (SEM). Ti-40Nb alloy served as a reference for comparison. The results demonstrated a significantly higher weight gain (3.37%) in TiH_2-40Nb alloy compared to Ti-40Nb alloy (1.99%). This enhanced apatite formation was due to the emission of hydrogen from the alloy, which increased the pH from 7.4, creating a more favorable alkaline environment for apatite precipitation. The local pH observed for the Ti-40Nb alloy and TiH_2-40Nb alloy were 8.24 and 8.30, respectively. As a conclusion, the role of hydrogen in enhancing the apatite formation, suggesting that TiH_2-based alloys could offer a cost-effective and bioactive alternative for implant materials.

Keywords: Beta phase titanium alloy implant; Hydrogen induced apatite formation; Mechanical alloying; Powder metallurgy; TiH_2-40Nb alloy

1. Introduction

The need for bone implants is increasing as a result of factors such as aging population, rapid socioeconomic development, and an increase in fracture incidents caused by traffic accidents, accidental injuries and osteoporosis in the elderly population. Bones, the most prevalent hard tissues in the human body, play a vital role as the main load-bearing structures, making their health essential for general physical well-being.

Bone implants used in clinical therapy are categorized into non-degradable implants like titanium (Ti) alloy, stainless steel as well as cobalt-based alloy. Meanwhile, degradable implants include magnesium (Mg) and iron (Fe) alloys. Among the non-degradable options, Ti as well as its alloys are widely utilized in the production of bone implants[1)].

Low stiffness is a requirement for bone implants, necessitating materials with a minimum Young's modulus (<30 GPa), combined with high strength (70-280 MPa)[2)]. The (α+β)-alloy Ti-6Al-4V alloy, featuring a Young's modulus of 110 GPa, is frequently chosen for bone implants due to its 1000 MN/m² strength and 40% greater resistance to corrosion than commercially pure titanium (cp-Ti), which has a Young's modulus of 105 GPa[3,4)]. The Ti-6Al-4V alloy, comprising 6 wt.% aluminum and 4 wt.% vanadium, is highly favored for load-bearing uses like hip, spinal as well as knee implants due to its remarkable strength[5)]. In contrast, commercially pure titanium (cp-Ti) offers lower mechanical properties because of its single-phase structure[6)]. Consequently, it makes it more appropriate for non-load-bearing applications like fixation mini plates and screws in craniofacial and maxillofacial procedures[7)]. However, both cp-Ti and Ti-6Al-4V possess a high Young's modulus, which greatly exceeds natural bone (<30 GPa), resulting in stress shielding effects[8,9)]. This discrepancy may cause bone loss as well as instability of the implant, ultimately leading to implant failure. Apart from that, releasing aluminum (Al) as well as vanadium

Cite: A. Farrahnoor et al., "TiH_2-40Nb Alloy as Alternative to Ti-40Nb Alloy for Bone Implant: A Comparative Study". Evergreen, 13 (03) 1025-1032 (2026). https://doi.org/10.5109/7439394.

(V) ions from Ti-6Al-4V alloy may potentially cause neurotoxic effects, Alzheimer's disease and cancer[10,11].

To address this issue, β-type Ti-based alloys, such as those in the titanium-niobium (Ti-Nb) system, have attracted significant attention because of their reduced Young's modulus, good corrosion resistance, higher strength, non-toxic, and superior biocompatibility[12,13]. The addition of Nb lowers the alloy's modulus by approximately 24%, which helps to better match the mechanical properties concerning bone[14-16]. Within the metastable Ti-Nb alloy system, two distinct compositions stand out with exceptionally low Young's modulus values, a crucial characteristic for minimizing stress shielding in bone implants: one with a Nb content ranging from 14-18 wt.% and another with approximately 40-45 wt.%[17]. Ti-Nb alloys containing 30–45 wt.% Nb are considered promising for bone implants, as their low Young's modulus (~50 GPa) closely aligns with that of natural bone[18]. Guo et al.[19] and Fikeni[20] emphasized that the β-phase remains fully stable when the Nb content exceeds 30 wt.%. Ti-40Nb alloy exhibits a predominantly β-phase microstructure (approximately 89%), contributing to the desirable mechanical properties for implant applications[21]. These results underscore the promise of Ti-Nb alloys, especially those with elevated Nb levels, in minimizing stress shielding and enhancing the effectiveness of bone implants.

Apart from that, the occurrence of Nb transforms the passivated Ti surface into a bioactive one by enhancing its ability to form apatite[22]. Wang et al.[23] indicated that the Ti-25Nb alloy possessed the minimal modulus of 18.7 ± 1.4 GPa, attributed to its high β phase content. Interestingly, this composition also showed the highest level of apatite formation among Ti-Nb alloys, indicating that the β-phase has a strong capability to enhance apatite growth. In another study, Gostin et al.[24] claimed that Ti-45Nb alloy showed a lower ability to form apatite compared to Ti. This disparity suggests that the relationship between Nb content, β phase stability, and apatite formation is not fully understood and requires further investigation.

Titanium hydride (TiH_2) offers a significant cost advantage over commercially pure titanium (cp-Ti), making it an attractive alternative where cost-effectiveness is a priority. This is due to the simpler and less energy-intensive production process of TiH_2 compared to the complex and costly methods required for producing cp-Ti[25,26]. Numerous studies have employed TiH_2 as a starting material for preparing Ti alloys, specifically β-phase stabilized Ti alloys, with a focus on investigating their mechanical properties. In Sharma et al.[27], a blend of cp-Ti, TiH_2, and Nb elemental powders was processed utilizing mechanical alloying, followed by a two-stage spark plasma sintering technique. Their research revealed that increasing the amount of TiH_2 powder mitigated powder agglomeration and sticking during milling, resulting in a higher yield of mechanically alloyed powder. Additionally, a notable reduction in the milled powder's particle size was observed as the TiH_2 content increased, leading to enhanced strength in the final alloy. In another study, Robertson and Schaffer[28] noted that the compressibility of the hydride is expected to improve considerably due to decreased cold welding and friction in the hydrogenated Ti-40Nb powders, a phenomenon previously noted in TiH_2. Dehydrogenation can create lattice defects and alter surface properties, thereby enhancing bioactivity by providing more reactive sites and increasing surface roughness that favor apatite formation[29,30]. Dehydrogenation also can promote the formation of Ti-OH groups, which play an important role in apatite nucleation[31]. These hydroxyl groups interact with inorganic ions in physiological solution, forming intermediates such as calcium titanate that subsequently attract phosphate ions, ultimately facilitating apatite layer growth[32,33]. The β phase of Ti, which remains stable at higher temperatures than the α phase, may also influence apatite formation. This phase offers distinct mechanical such as a lower modulus, which can also affect the interaction between Ti surfaces and biological environments. Although direct studies on the β phase's role in apatite formation are limited, its phase transformation could impact apatite binding and growth by altering surface energy and the density of active sites available for nucleation[34,35]. Despite the recognized potential of TiH_2 in improving the mechanical characteristics of Ti alloys, there exists a gap on the interaction of the Ti-Nb system with hydrogen to influence the formation of bone-like apatite. Hence, information on the effect of dehydrogenation on β-type Ti-based alloys is currently scarce in the literature. In contrast, it is anticipated that TiH_2-40 Nb alloys, particularly when tailored for enhanced apatite-forming ability will emerge as a future alternative to conventional alloys for bone implant applications, given the promising outcomes demonstrated in this comparative study.

Powder metallurgy is a reliable technique for the near net-shape fabrication of bone implant applications. One of its key benefits is the precise control it provides over the chemical composition of the material, enabling customization of properties to suit particular needs. In addition, this method enhances the feasibility of producing complex shapes with high precision, which is crucial for implant applications. Powder metallurgy also reduces overall production costs, making it a cost-effective solution for manufacturing high-quality, custom implants. These combined benefits make powder metallurgy a highly attractive option for the development of bone implants[36-39].

Despite these advancements, limited studies have focused on the effect of hydrogen on the Ti-Nb system, particularly

its role in influencing apatite formation and implant integration. Since Nb stabilizes the β-phase, its interaction with hydrogen is expected to alter the apatite-forming ability of the alloy in ways that differ from Ti-Nb alloys. This study addresses that gap by investigating the comparative behavior of Ti-40Nb and TiH₂-40Nb alloys fabricated through mechanical alloying and powder metallurgy methods. The apatite formation, pH, and microstructure of the Ti-40Nb alloy and TiH₂-40Nb alloy are compared, and the findings related to these aspects are presented and discussed. The novelty of this research lies in its combined focus on hydrogenated Ti as a cost-effective precursor and its role in tailoring the bioactive properties of β-phase Ti-Nb alloys for bone implant applications.

2. Materials and Methods

2.1. Raw materials

For all experiments, mixtures of Ti, TiH_2 and Nb were prepared from highly pure starting powders: 99.7% Ti (Strem), 98% TiH_2 (Merck), and 99.8% Nb (Strem). These mixtures reacted to form stoichiometric Ti-40Nb alloy and TiH₂-40Nb alloy, as detailed in Table 1.

2.2. Preparation of pre-alloyed powders

Sample preparation involved a multi-stage process, encompassing mechanical alloying, powder metallurgy, compaction, and sintering process, for synthesizing β-phase stabilized titanium-based alloys utilizing a combination of Ti and TiH₂ powders as the initial material, as shown in Figure 1. The mechanical milling process was carried out with a Fritsch Pulverisette P-5 planetary ball mill, equipped with four 250 ml stainless steel vials. The milling process was conducted for 2 hours at a speed of 200 rpm, using a typical 10:1 ball-to-powder ratio with 10 mm stainless steel balls and n-heptane as the process control agent. To avoid oxidation, argon gas was used to purge the milling vials before milling began. The resulting pre-alloyed powders were then compacted into disc-shaped green pellets using a Specac manual hydraulic press at a pressure of 500 MPa. These pellets were sintered in a Lenton tube furnace at 1200 °C for 3 hours under an argon atmosphere. The heating and cooling rates were both maintained at 10 °C/min, with furnace cooling applied afterward, as illustrated in Figure 2.

Table 1: Specification of elemental powders and powder mixture

Alloy composition	Ti powder (wt.%)	TiH₂ powder (wt.%)	Nb powder (wt.%)
Ti-40Nb	60	None	40
TiH₂-40Nb	None	60	40

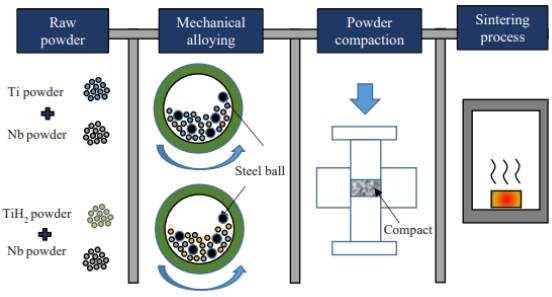

Fig. 1: Integrating mechanical alloying with powder metallurgy for producing Ti-40Nb alloy and TiH₂-40Nb alloy

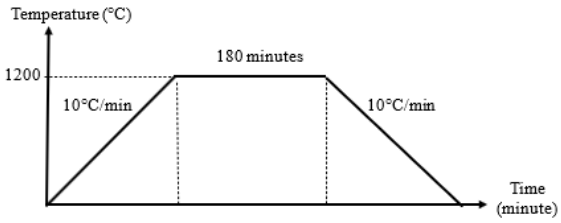

Fig. 2: Sintering profile of Ti-40Nb alloy and TiH₂-40Nb alloy

2.3. Testing and Characterizations

Thermogravimetric analysis (TGA) was performed using a Perkin Elmer (M) 1 analyser, with samples heated from room temperature to 900 °C at 10 °C/min under a nitrogen flow of 10 mL/min.

The samples' in-vitro bioactivity was evaluated by soaking them in Hank's Balanced Salt Solution (HBSS) with a maintained pH of 7.4. This immersion aimed to simulate the physiological conditions of the human body as well as evaluate the ability of the alloys to induce apatite formation, a key indicator of bioactivity. Each sample was immersed in 30 mL of HBSS solution in a polyethylene (PE) bottle, as shown in Figure 3. The bottles were then positioned in a water bath (model: TWB-30D, 30L), maintained at a temperature of 37 °C for a duration of 30 days.

Following the 30-day immersion period, the samples were carefully retrieved from the HBSS solution and thoroughly dried in a desiccator containing silica gel for four days. The weight gain of each sample, a direct measure of apatite formation, was then calculated using the following formula, as shown in Equation 1.

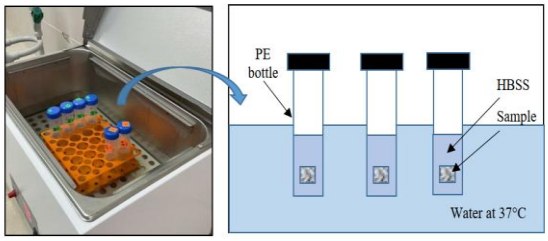

Fig. 3: Schematic diagram of samples in a water bath for an immersion test

Cite: A. Farrahnoor et al., "TiH₂-40Nb Alloy as Alternative to Ti-40Nb Alloy for Bone Implant: A Comparative Study". Evergreen, 13 (03) 1025-1032 (2026). https://doi.org/10.5109/7439394.

$$Weight\ gain\ (\%) = \frac{W_F - W_I}{W_F}\ x\ 100 \qquad (1)$$

in which W_I refers to the initial dry weight of the sample prior to the immersion, while W_F refers to the final dry weight post 30-day immersion in HBSS solution.

Scanning Electron Microscopy (SEM) with a Hitachi TM3030Plus Tabletop Microscope was utilized to examine the surface morphology of the samples. This high-resolution imaging technique allowed for detailed visualization of the apatite layer created on the alloy's surfaces.

The changes in pH of the HBSS solutions after sample immersion were also monitored. A pH meter manufactured by Hanna Instruments was used for this purpose. To ensure accuracy, the pH meter was calibrated before each measurement using three standard solutions with pH values of 4, 7, and 10. During measurement, the pH meter probe was inserted into the HBSS solution to a depth of no more than 1 mm and held until a stable pH reading was obtained. Each measurement was repeated three times at 5-minute intervals to ensure consistency and reliability of the data.

3. Results and Discussions

3.1. Thermogravimetric analysis (TGA)

The TGA curve exhibited negligible weight change in the initial heating stage (0-300 °C), indicating that TiH_2 remained stable and no significant hydrogen release occurred (Figure 4). Noticeable weight loss began at higher temperatures, around 340-410 °C, marking the onset of dehydrogenation[40,41]. The controlled release of hydrogen during heating not only densifies the alloy but also introduces microstructural defects that remain embedded in the final materials. These defects act as preferential sites for Ti-OH formation, enhancing the alloy's ability to induce apatite deposition once exposed to HBSS solution.

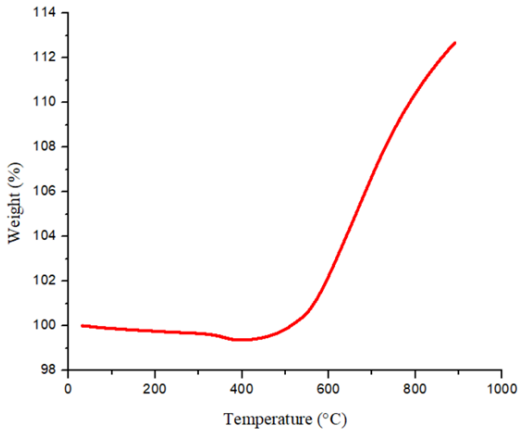

Fig. 4: TGA of TiH_2-40Nb alloy during milling at 200 rpm

3.2. Weight gain and pH measurement

Figure 5 illustrates a notable difference in both pH and weight gain of apatite formed on TiH_2-40Nb alloy and Ti-40Nb alloy after 30 days of immersion in HBSS solution. Both alloys showed a slight increase in pH above the neutral value (7.4) of HBSS solution. The slightly higher pH for TiH_2-40Nb alloy (8.30) compared to Ti-40Nb alloy (8.24) indicated a more pronounced alkaline environment in the surrounding solution, which was conducive to apatite formation. The slight increase in pH observed for the TiH_2-40Nb alloy could be attributed to the interaction of the alloy with HBSS solution. This alkaline shift was attributed to the decomposition of TiH_2-40Nb alloy in an aqueous environment, releasing hydrogen ions (H^+) that subsequently react with dissolved oxygen in HBSS solution to produce water (H_2O) and hydroxide ions (OH^-). This phenomenon is supported by studies from Udduttula et al.[42], who reported that an alkaline pH enhances apatite formation on metallic bio-implants when immersed in physiological solutions. The enhanced alkalinity observed in TiH_2-40Nb alloy can be attributed to surface modification introduced during hydrogenation-dehydrogenation which increase the density of Ti-OH groups that drive ion exchange.

The present study demonstrated that the TiH_2–40Nb alloy exhibited substantially enhanced apatite-forming ability compared to the Ti–40Nb alloy, as evidenced by a markedly higher weight gain of 3.37% versus 1.99%, respectively. This difference is particularly noteworthy given that apatite is known to precipitate more readily under alkaline conditions[34], and the elevated pH measured in the vicinity of the TiH_2–40Nb alloy provides a favorable thermodynamic environment for apatite nucleation and growth. The alignment between the pH findings and the weight gain results strongly suggests that the local alkaline environment generated by hydrogen incorporation played a significant role in driving apatite deposition.

Beyond its influence on pH, hydrogen in the TiH_2–40Nb alloy also contributed to the modifications in surface

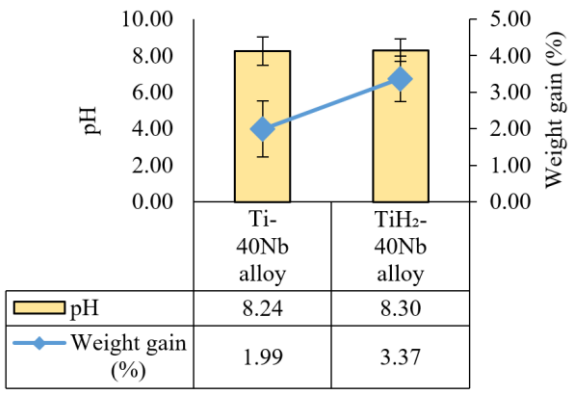

Fig. 5: pH measurement and weight gain of Ti-40Nb alloy and TiH_2-40Nb alloy after 30 days of immersion in HBSS solution

chemistry. Specifically, hydrogen altered the native oxide layer, increasing surface reactivity and promoting the adsorption of calcium ions (Ca^{2+}) and phosphate ions (PO_4^{3-}) which are the primary ionic constituents of apatite[35]. This in turn creates a more bioactive surface conducive to mineral deposition and growth. These observations are consistent with the findings of Combes et al.[43] and Ghodrati et al.[44], who reported that hydrogen-modified Ti surfaces exhibited altered oxide defect structures and increased hydroxyl group density, which further enhanced calcium phosphate nucleation kinetics.

Phase composition analysis further contextualizes these findings. As reported in our previous study[45], the Ti–40Nb alloy comprised 34.3% α-Ti and 65.7% β-Ti, a phase distribution comparable to that of the TiH₂–40Nb alloy (34% α-Ti and 66% β-Ti), confirming that both alloys are predominantly β-phase in character. The β-phase is well-established to influence the mechanical and surface properties of Ti-based alloys, notably by reducing the elastic modulus and improving biocompatibility through enhanced surface stability and favorable oxide formation, which supports ion exchange and interfacial reactivity[46]. Given this near-equivalent β-phase constitution, the observed differences in bioactivity between the two alloys cannot be attributed to phase composition alone.

Collectively, these findings indicate that while both alloys share a similar and predominantly β-phase microstructure (~66%), the substantially enhanced apatite-forming ability of the TiH₂–40Nb alloy is principally governed by hydrogen-induced surface and chemical modifications rather than by differences in phase distribution. This supports the conclusion that hydrogen-assisted processing plays a dominant and decisive role in enhancing the bioactivity of Ti–Nb alloys.

3.3. Morphological observation

As shown in Figure 6, the surface morphology of Ti-40Nb and TiH₂-40Nb alloys differs after 30 days of immersion in HBSS, with the micrographs displaying varying degrees of apatite development on each alloy. The Ti-40Nb alloy surface appeared coarse and uneven in texture, partially covered with small apatite deposits, indicating limited bioactivity in terms of apatite nucleation and growth. This is consistent with observations reported by Farrahnoor and Zuhailawati[13] who found that Ti-40Nb alloy immersed in HBSS solution exhibited low and scattered distributions of Ca, P, and O elements across the surface as revealed by SEM-EDS mapping. In contrast, the surface of TiH₂-40Nb alloy displayed a finer grain structure caused by the occurrence of TiH_2, which enhances the formation of oxide layer that smoothens surface irregularities. Upon exposure to HBSS solution, releasing hydrogen ions (H^+) from TiH_2 raises the local concentration of H^+ in the surrounding environment. This leads to a shift towards a more alkaline (higher pH), which in turn attracts calcium ions (Ca^{2+}) and phosphate ions (PO_4^{3-}). The occurrence of these ions in the alkaline solution promotes the deposition and growth of apatite on the TiH₂-40Nb alloy surface. This suggests that the TiH₂-40Nb alloy has a higher bioactivity, promoting more extensive apatite nucleation and growth. The morphological analysis aligned well with the in-vitro apatite formation and pH findings.

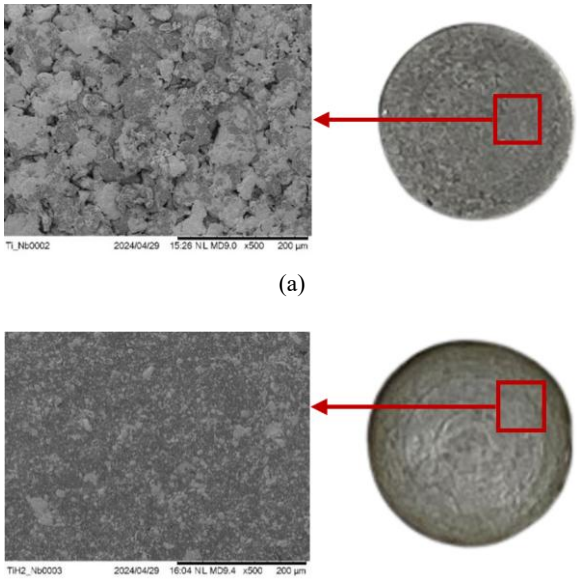

Fig. 6: SEM micrographs indicating surface appearance of different Ti alloys post immersion in HBSS solution for 30 days at 37 °C: a) Ti-40Nb alloy, and b) TiH₂-40Nb alloy at magnification of 500x

4. Conclusions

The TiH₂-40Nb alloy demonstrated superior performance, exhibiting a significantly higher weight gain due to apatite formation (3.37%) compared to Ti-40Nb alloy (1.99%). Similarly, the TiH₂-40Nb alloy produced a slightly more alkaline environment (pH 8.30) than Ti-40Nb alloy (pH 8.24), which is favorable for apatite nucleation and growth. SEM analysis further confirmed denser and more uniform apatite coverage on the TiH₂-40Nb alloy, indicating enhanced apatite-forming ability facilitated by hydrogen's influence on surface chemistry and oxide layer modification.

From an application perspective, TiH₂-40Nb alloy offers a cost-effective and bioactive alternative to Ti-Nb alloy, making it a promising candidate for bone implant applications, particularly in load-bearing conditions.

Future work should include surface chemistry characterization using XPS and FTIR to confirm the hydrogen-induced Ti–OH group formation and oxide layer modifications along with residual hydrogen quantification via thermal desorption spectroscopy. Meanwhile, characterization of the deposited apatite layer should also be conducted, including XRD analysis to identify crystalline phases, SEM-EDS elemental mapping to

confirm calcium and phosphorus distribution, Ca/P ratio quantification and Raman spectroscopy or XPS to verify the chemical composition of the deposited layer. Additionally, in-vitro biological evaluation and optimization of hydrogen concentration should be pursued to validate the biological response and balance bioactivity with long-term mechanical stability.

Acknowledgements

This study received funding from the Ministry of Higher Education Malaysia under grant number FRGS/1/2021/TK0/UITM/02/35. The authors also extend their gratitude to Universiti Teknologi MARA Cawangan Pulau Pinang for providing the technical assistance and facilities needed to complete this study.

References

1) Y.-W. Cui, L. Wang, and L.-C. Zhang, "Towards load-bearing biomedical titanium-based alloys: From essential requirements to future developments," Prog. Mater. Sci., 144 101277 (2024). doi:10.1016/j.pmatsci.2024.101277.
2) C. Liao, Y. Li, and S.C. Tjong, "Polyetheretherketone and its composites for bone replacement and regeneration," Polymers, 12 (12) 2858 (2020). doi:10.3390/polym12122858.
3) F.N. Depboylu, E. Yasa, Ö. Poyraz, J. Minguella-Canela, F. Korkusuz, and M.A.D. los Santos López, "Titanium based bone implants production using laser powder bed fusion technology," J. Mater. Res. Technol., 17 1408–1426 (2022). doi:10.1016/j.jmrt.2022.01.087.
4) A. Saini, B.S. Pabla, and S.S. Dhami, "Developments in cutting tool technology in improving machinability of Ti6Al4V alloy: A review," Proc. Inst. Mech. Eng. B J. Eng. Manuf., 230 (11) 1977–1989 (2016). doi:10.1177/0954405416640176.
5) S.L. Campanelli, N. Contuzzi, A.D. Ludovico, F. Caiazzo, F. Cardaropoli, and V. Sergi, "Manufacturing and characterization of Ti6Al4V lattice components manufactured by selective laser melting," Materials, 7 (6) 4803–4822 (2014). doi:10.3390/ma7064803.
6) N.U. Navi, J. Tenenbaum, E. Sabatani, G. Kimmel, R. Ben David, B.A. Rosen, Z. Barkav, V. Ezersky, E. Tiferet, Y.I. Ganor, and N. Eliaz, "Hydrogen effects on electrochemically charged additive manufactured by electron beam melting (EBM) and wrought Ti–6Al–4V alloys," Int. J. Hydrogen Energy, 45 (46) 25523–25540 (2020). doi:10.1016/j.ijhydene.2020.06.277.
7) D.M. Brunette, "Principles of cell behavior on titanium surfaces and their application to implanted devices," Titanium in Medicine, Springer, Berlin, Heidelberg, pp. 485–512 (2001). doi:10.1007/978-3-642-56486-4_15.
8) S.F. Jawed, C.D. Rabadia, M.A. Khan, and S.J. Khan, "Effect of alloying elements on the compressive mechanical properties of biomedical titanium alloys: A systematic review," ACS Omega, 7 (34) 29526–29542 (2022). doi:10.1021/acsomega.2c02096.
9) E. Liverani, G. Rogati, S. Pagani, S. Brogini, A. Fortunato, and P. Caravaggi, "Mechanical interaction between additive-manufactured metal lattice structures and bone in compression: Implications for stress shielding of orthopaedic implants," J. Mech. Behav. Biomed. Mater., 121 104608 (2021). doi:10.1016/j.jmbbm.2021.104608.
10) G. Khadija, A. Saleem, Z. Akhtar, Z. Naqvi, M. Gull, M. Masood, S. Mukhtar, M. Batool, N. Saleem, T. Rasheed, N. Nizam, A. Ibrahim, and F. Iqbal, "Short term exposure to titanium, aluminum and vanadium (Ti 6Al 4V) alloy powder drastically affects behavior and antioxidant metabolites in vital organs of male albino mice," Toxicol. Rep., 5 765–770 (2018). doi:10.1016/j.toxrep.2018.06.006.
11) A. Azmat, S. Asrar, I.A. Channa, J. Ashfaq, I.A. Chandio, A.D. Chandio, M.A. Shar, M.S. AlSalhi, and S. Devanesan, "Comparative study of biocompatible titanium alloys containing non-toxic elements for orthopedic implants," Crystals, 13 (3) 467 (2023). doi:10.3390/cryst13030467.
12) A. Maciej, M. Marny, M. Sowa, A. Blacha-Grzechnik, A. Stolarczyk, J. Michalska, and W. Simka, "Microstructure and corrosion resistance of Ti and Ti-40Nb alloy modified by plasma electrolytic oxidation in tricalcium phosphate suspension," Electrochim. Acta, 468 143185 (2023). doi:10.1016/j.electacta.2023.143185.
13) A. Farrahnoor, and H. Zuhailawati, "Effects of hydroxyapatite addition on the bioactivity of Ti-Nb alloy matrix composite fabricated via powder metallurgy process," Mater. Today Commun., 27 102209 (2021). doi:10.1016/j.mtcomm.2021.102209.
14) Y. Okazaki, "A new Ti-15Zr-4Nb-4Ta alloy for medical applications," Curr. Opin. Solid State Mater. Sci., 5 (1) 45–53 (2001). doi:10.1016/S1359-0286(00)00025-5.
15) Y. Marsumi, and A.W. Pramono, "Influence of niobium or molybdenum in titanium alloy for permanent implant application," Adv. Mater. Res., 900 53–63 (2014). doi:10.4028/www.scientific.net/AMR.900.53.
16) G.C. Cardoso, G.S. de Almeida, D.O.G. Corrêa, W.F. Zambuzzi, M.A.R. Buzalaf, D.R.N. Correa, and C.R. Grandini, "Preparation and characterization of novel as-cast Ti-Mo-Nb alloys for biomedical applications," Sci. Rep., 12 11874 (2022). doi:10.1038/s41598-022-14820-8.

17) T. Ozaki, H. Matsumoto, S. Watanabe, and S. Hanada, "Beta Ti alloys with low Young's modulus," Mater. Trans., 45 (8) 2776–2779 (2004). doi:10.2320/matertrans.45.2776.
18) A. Farrahnoor, and H. Zuhailawati, "Review on the mechanical properties and biocompatibility of titanium implant: The role of niobium alloying element," Int. J. Mater. Res., 112 (6) 505–513 (2021). doi:10.1515/ijmr-2020-8060.
19) S. Guo, Y. Shi, G. Liu, R. Wu, R. Luo, C.T. Peng, Q. Meng, X. Cheng, X. Zhao, and X. Zhao, "Design and fabrication of a (β+α") dual-phase Ti-Nb-Sn alloy with linear deformation behavior for biomedical applications," J. Alloys Compd., 805 517–521 (2019). doi:10.1016/j.jallcom.2019.07.109.
20) L. Fikeni, "Microstructural evolution and its influence on mechanical properties of TiNb binary alloys," MSc Thesis, University of Pretoria, Republic of South Africa, pp. 1–96 (2021).
21) A. Farrahnoor, and H. Zuhailawati, "A brief review on the properties of titanium as a metallic biomaterial," Int. J. Electroactive Mater., 8 63–67 (2020).
22) V.P. Ricci, C.R.M. Afonso, R.F.M. dos Santos, A.M.J. Junior, and V. Roche, "Anodic growth and pre-calcification on β-Ti-40Nb alloy: Effects on elastic modulus, electrochemical properties, and bioactivity," Ceram. Int., 48 (19) 27575–27589 (2022). doi:10.1016/j.ceramint.2022.06.052.
23) Q. Wang, C. Han, T. Choma, Q. Wei, C. Yan, B. Song, and Y. Shi, "Effect of Nb content on microstructure, property and in vitro apatite-forming capability of Ti-Nb alloys fabricated via selective laser melting," Mater. Des., 126 268–277 (2017). doi:10.1016/j.matdes.2017.04.026.
24) P.F. Gostin, A. Helth, A. Voss, R. Sueptitz, M. Calin, J. Eckert, and A. Gebert, "Surface treatment, corrosion behavior, and apatite-forming ability of Ti-45Nb implant alloy," J. Biomed. Mater. Res. Part B, 101 (2) 269–278 (2013). doi:10.1002/jbm.b.32836.
25) A.F. Sa'adi, A. Farrahnoor, and H. Zuhailawati, "Influence of processing parameters on dehydrogenation of TiH_2 in the preparation of Ti–Nb: A review," Heliyon, 8 (11) e11602 (2022). doi:10.1016/j.heliyon.2022.e11602.
26) S.M. Hosnie, M. Yahaya, N.A. Haris, and M.H. Ismail, "Thermal analysis and microstructural study of porous β-TiNb incorporated with TiH_2 powder via low-cost processing route," J. Adv. Manuf. Technol., 12 (2) 121–131 (2018).
27) B. Sharma, S.K. Vajpai, and K. Ameyama, "An efficient powder metallurgy processing route to prepare high-performance β-Ti–Nb alloys using pure titanium and titanium hydride powder," Metals, 8 (7) 516 (2018). doi:10.3390/met8070516.
28) I.M. Robertson, and G.B. Schaffer, "Comparison of sintering of titanium and titanium hydride powders," Powder Metall., 53 (1) 12–19 (2010). doi:10.1179/003258909X12450768327063.
29) Z. Li, Q. Tang, Z. Huang, Q. Liu, X. Wang, J. Li, G. Yin, Y. Bai, and F. Chen, "Digital light processing of Ti_xO_y@Ti/HA biomaterials by oxidation of TiH_2 and dehydrogenation of TiO_2@TiH_2/HA precursors," J. Am. Ceram. Soc., 107 (7) 4478–4493 (2024). doi:10.1111/jace.19796.
30) C. Reynaud, C. Thomas, D. Brouri, J. Schnee, S. Casale, and G. Costentin, "Oxidative dehydrogenation of propane on hydroxyapatite-supported cobalt catalysts," ChemCatChem, 17 (10) e202402100 (2025). doi:10.1002/cctc.202402100.
31) T. Zheng, C. Wu, Y. Zhang, M. Chen, and P.T. Cummings, "Molecular investigation of the initial nucleation of calcium phosphate on TiO_2 substrate: The effects of surface nanotopographies," Cryst. Growth Des., 18 (6) 1205–1215 (2018). doi:10.1021/acs.cgd.8b00123.
32) J. Fan, P. Wang, S. Wang, R. Li, Y. Yang, L. Jin, Y. Sun, and D. Li, "Advances in macro-bioactive materials enhancing dentin bonding," Discov. Nano, 20 (1) 40 (2025). doi:10.1186/s11671-025-04206-w.
33) R. Kumar, U. Topno, D. Shikha, S. Anand, S.K. Sinha, P.K. Mohanty, and S. Mhaske, "High antioxidant activity, enhanced cytocompatibility, improved apatite formation, and moderate thrombogenicity of copper-doped hydroxyapatite attributed to structural changes analysed using EDX, FTIR, XRD, and FESEM," BioNanoSci., 15 323 (2025). doi:10.1007/s12668-025-01984-6.
34) R. Huang, W. Suo, Y. Wang, Y. Pan, G. Ren, H. Hu, and L. Huang, "Enhancing wear resistance, anti-corrosion property and surface bioactivity of a beta-titanium alloy by adopting surface mechanical attrition treatment followed by phosphorus ion implantation," Appl. Surf. Sci., 671 160766 (2024). doi:10.1016/j.apsusc.2024.160766.
35) S.L. Sing, "Perspectives on additive manufacturing enabled beta-titanium alloys for biomedical applications," Int. J. Bioprint., 8 (1) 478 (2022). doi:10.18063/ijb.v8i1.478.
36) K. Munir, A. Biesiekierski, C. Wen, and Y. Li, "Powder metallurgy in manufacturing of medical devices," Metallic Biomaterials Processing and Medical Device Manufacturing, Woodhead Publishing, pp. 159–190 (2020). doi:10.1016/B978-0-08-102965-7.00005-9.
37) A. Laptev, A.P.C. Barbosa, N. Daudt, and M. Bram, "Review of the powder metallurgical production of net-shaped titanium implants," Key Eng. Mater., 704 311–317 (2016). doi:10.4028/www.scientific.net/KEM.704.311.

Cite: A. Farrahnoor et al., "TiH_2-40Nb Alloy as Alternative to Ti-40Nb Alloy for Bone Implant: A Comparative Study". Evergreen, 13 (03) 1025-1032 (2026). https://doi.org/10.5109/7439394.

38) M.M. Dewidar, H.-C. Yoon, and J.K. Lim, “Mechanical properties of metals for biomedical applications using powder metallurgy process: A review,” Met. Mater. Int., 12 (3) 193–206 (2006). doi:10.1007/BF03027531.
39) A.M. Abraham, and S. Venkatesan, “A critical review on biomaterials using powder metallurgy method,” Eng. Res. Express, 6 (1) 012508 (2024). doi:10.1088/2631-8695/ad35a6.
40) T. Hu, M. Lin, J. Zou, W. Wang, W. Ji, and Z. Fu, “Pressure-controlled synergy between dehydrogenation and densification in TiH_2 sintering,” J. Eur. Ceram. Soc., 45 (14) 117551 (2025). doi:10.1016/j.jeurceramsoc.2025.117551.
41) N.U. Navi, B.A. Rosen, E. Sabatani, J. Tenenbaum, E. Tiferet, and N. Eliaz, “Thermal decomposition of titanium hydrides in electrochemically hydrogenated electron beam melting (EBM) and wrought Ti–6Al–4V alloys using in situ high-temperature X-ray diffraction,” Int. J. Hydrogen Energy, 46 (59) 30423–30432 (2021). doi:10.1016/j.ijhydene.2021.06.166.
42) A. Udduttula, J. Li, Z. Ma, B. Teng, J.V. Zhang, A.M. Ferreira, P. Gentile, G. Wang, X. Zhao, and P.-G. Ren, “A novel apatite-inspired $Sr_5(PO_4)_2SiO_4$ plasma-sprayed coating on Ti alloy promoting biomineralization, osteogenesis and angiogenesis,” Ceram. Int., 48 (8) 10979–10989 (2022). doi:10.1016/j.ceramint.2021.12.317.
43) C. Combes, C. Rey, and M. Frèche, “XPS and IR study of dicalcium phosphate dihydrate nucleation on titanium surfaces,” Colloids Surf. B: Biointerfaces, 11 (1–2) 15–27 (1998). doi:10.1016/S0927-7765(98)00014-9.
44) H. Ghodrati, A. Goodarzi, M. Golrokhian, F. Fattahi, R. Mahmoudi Anzabi, M. Mohammadikhah, S. Sadeghi, and S. Mirhadi, “A narrative review of recent developments in osseointegration and anti-corrosion of titanium dental implants with nano surface,” Bone Rep., 25 101846 (2025). doi:10.1016/j.bonr.2025.101846.
45) A.F. Sa’aidi, H. Zuhailawati, and A. Farrahnoor, “Optimisation of TiH_2–Nb alloy for bone implant using Box–Behnken design: Enhancing strength, elastic modulus and dehydrogenation behaviour through powder metallurgy,” Materialia, 45 102640 (2026). doi:10.1016/j.mtla.2025.102640.
46) J.V. Calazans Neto, C.A.S. Celles, C.S.A.F. de Andrade, C.R.M. Afonso, B.E. Nagay, and V.A.R. Barão, “Recent advances and prospects in β-type titanium alloys for dental implants applications,” ACS Biomater. Sci. Eng., 10 (10) 6029–6060 (2024). doi:10.1021/acsbiomaterials.4c00963.

Cite: A. Farrahnoor et al., "TiH_2-40Nb Alloy as Alternative to Ti-40Nb Alloy for Bone Implant: A Comparative Study". Evergreen, 13 (03) 1025-1032 (2026). https://doi.org/10.5109/7439394.